Chinese Journal of
POLYMER SCIENCE

RESEARCH ARTICLE

https://doi.org/10.1007/s10118-023-3054-8
Chinese J. Polym. Sci. **2024**, *42*, 333–343

Ion-conducting Membranes Based on Bacterial Cellulose Nanofibers Modified by Poly(sodium acrylate-*co*-2-acrylamido-2-methylpropanesulfonic acid)

Elizaveta V. Batishcheva*, Nikolay N. Smirnov, Natalya V. Bobrova, Maria P. Sokolova, and Michael A. Smirnov*

Institute of Macromolecular Compounds, Russian Academy of Sciences, Bolshoy pr. 31, Saint Petersburg 199004, Russia

Electronic Supplementary Information

Abstract Green method for preparation of ion-conducting membranes (ICM) based on bacterial cellulose nanofibers (CNF) modified by a copolymer of sodium acrylate and 2-acrylamido-2-methylpropanesulfonic acid was elaborated. FTIR and NMR data confirmed grafting of polyacrylate onto cellulose surface. Formation of porous structure of the ICM was controlled by SEM and AFM. The maximal ionic conductivity of the membranes reaches 1.5 and 3.1 mS·cm^{-1} (60 °C and 98% relative humidity) when they are saturated with water or H_2SO_4 (1 mol·L^{-1}) electrolyte, respectively. Prepared ICM was tested as a separator in a symmetrical supercapacitor with electrodes based on polyaniline hydrogel. The assembled cell demonstrate ability to operate at high current density up to 100 A·g^{-1} maintaining specific capacitance 165 F·g^{-1}. Maximal specific capacitance of 289 F·g^{-1} was achieved at current density 1 A·g^{-1}. Retaining of 90% of initial capacitance after 10000 of charge-discharge cycles proves high electrochemical stability of prepared ICM.

Keywords Bacterial cellulose; Ion conductivity; Porous membrane; Supercapacitor

Citation: Batishcheva, E. V.; Smirnov, N. N.; Bobrova, N. V.; Sokolova, M. P.; Smirnov, M. A. Ion-conducting membranes based on bacterial cellulose nanofibers modified by poly(sodium acrylate-*co*-2-acrylamido-2-methylpropanesulfonic acid). *Chinese J. Polym. Sci.* **2024**, *42*, 333–343.

INTRODUCTION

Due to increasing of energy consumption and growing number of portable devices, the development of eco-friendly and sustainable materials for energy storage[1,2] is an important scientific task of the modern science.[3] Thus, green materials are of high interest for application in batteries,[4,5] Li-ion power sources,[5–7] supercapacitors[8] and fuel cells.[9,10] All these devices use electrochemical processes on the electrode/electrolyte interface, while cathode and anode spaces are separated by the ion-conducting membrane (ICM).[11] Currently Nafion (DuPont) is the "gold standard" material for ICM[12] due to high ionic conductivity, chemical and mechanical stability. At the same time high cost, low operating temperature, low dimensional stability and hazardous preparation method are drawbacks of this material.[13] In this regard, searching for greener alternative materials for ICM is an actual task of modern science and technology. The main direction on this route is the elaboration of membranes based on biopolymers.[14] Biopolymers are cheaper[15] and easier to recycle and store, they are eco-friendly due to the possibility to decompose without elimination of hazardous molecules.[16] Polysaccharides, such as cellulose,[17] chitin,[18] chitosan,[19,20] alginate,[21] starch,[22] pectin,[23] agar[24] and their derivatives are the main objects that are studied as a components of future electrolyte membranes and electrodes in electrochemical energy storage devices.

Cellulose is the most abundant biopolymer,[25] which can be obtained from different sources such as plant biomass, agricultural waste, algae or can be produced by microorganisms like Acetobacter xylinum.[26] Bacterial cellulose (BC) attracts attention as a prospective material for membrane preparation[27] due to high mechanical strength,[28] good water retention, non-toxicity, chemical purity and biodegradability.[29] Exceptional capabilities of BC and its derivatives make this polymer prospective in various fields such as food industry,[30] biomedicine,[31] electronics,[32] fuel cell technology[33] and supercapacitors.[34,35] This unique nanostructured polymeric material is synthesized using simple culturing methods.[36] Unlike plant cellulose, BC does not contain lignin, hemicellulose, pectin, arabinose and other plant-derived contaminants.[37]

The way that is often used for preparation of BC based ICM is mixing it with other polymer that contains ionogenic groups. For example, membranes prepared by mixing of BC and Nafion with subsequent casting demonstrated heat resistance, high mechanical strength and exhibited the maximum

* Corresponding authors, E-mail: batischevaelisaveta@gmail.com (E.V.B.)
E-mail: smirnov_michael@mail.ru (M.A.S.)

Received July 22, 2023; Accepted September 12, 2023; Published online November 3, 2023

ionic conductivity of 71 mS·cm^{-1} at 30 °C and 100% relative humidity (RH).[38] By impregnation of Nafion dispersion into a 3D network of nanofibrillar BC ionic conductivity of 140 mS·cm^{-1} was achieved at 94 °C and RH=98%.[39] Although membranes based on BC/Nafion demonstrated reasonable properties, taking into account sustainable development goals the using of perfluorinated polymers should be avoided.

Additional benefit of cellulose is the availability of reactive hydroxyl groups on its surface. This allows chemical modification in order to introduce ionogenic groups providing the appearance of mobile ions inside the membrane and thus regulating of ionic conductivity.[17,40] The most common approaches towards modifying cellulose are 2,2,6,6-tetramethylpiperidine-1-oxyl-mediated oxidation,[41] phosphorylation,[42] carboxymethylation[43] and sulfonation.[44] Different types of sulfonation have been employed to enhance the ionic conductivity of cellulose based ICM. Impregnation of a membrane based on CNF with sulfosuccinic acid allow to achieve ionic conductivity 3.17 mS·cm^{-1}.[45] Sulfonation of cellulose with sodium bisulfite result in obtaining of a membrane with conductivity of 2 mS·cm^{-1} at 120 °C.[15]

The widely used industrial sulphonated polymer is prepared by polymerization of 2-acrylamido-2-methyl-1-propanesulfonic acid (AMPS) and attracts much attention due to its very high degree of dissociation, low price, non-toxicity, hydrolytic stability and swelling behavior.[46] Cellulose modified with this polymer was used for obtaining of superabsorbent materials.[46,47] However, these sorbents were prepared in the form of blocks with cross-linker (*N*,*N*′-methylenebisacrylamide) that does not allow to evaluate chemical grafting of polyacrylate to cellulose surface. It can be proposed that chemical grafting of sulphonated polyacrylate can be used for enhancing of ionic conductivity of cellulose-based materials along with attaining high stability of membrane composition. For the best of our knowledge, the preparation and electrochemical performance of cellulose-based membranes with proved covalent grafting of sulphonated polyacrylate were not reported yet. Thus, the aim of this work was to fill this gap and for the first time demonstrate the approach for preparation of porous ICM based on CNF that are modified by grafting of copolymer of sodium acrylate and AMPS using cerium (IV) ammonium nitrate as initiator. The structure of modified CNF and membranes based on them as well as their electrochemical properties have been investigated. Additionally, the performance of prepared membranes as a separator in the symmetrical supercapacitor with polyaniline hydrogel-based electrodes has been demonstrated.

EXPERIMENTAL

Materials

The lyophilized culture of A. xylinum was purchased from the All-Russian collection of industrial microorganisms (National Bioresource Center, GosNIIgenetics, Moscow, Russia) and cultured. Peptone and D-mannitol (CAS 69-65-8) were obtained from LenReaktiv (Saint Petersburg, Russia). Choline chloride (ChCl) (Glentham Life Sciences Ltd., Corsham, UK, CAS 67-48-1, purity>99%) was dried under vacuum at 60 °C for at least 24 h before use. Urea (LenReactiv, Saint Petersburg, Russia, CAS 57-13-6, purity 98%). AMPS (CAS 15214-89-8) and acrylic acid (AA) (CAS 607-061-00-8, purity >99%) were purchased from Merck, German and from Sigma-Aldrich, Czech Republic, respectively. Cerium (IV) ammonium nitrate ($(NH_4)_2Ce(NO_3)_6$) (Merck, German, CAS16774-21-3), nitric acid (HNO_3) (Vekton, Saint Petersburg, Russia, CAS 7697-37-2) and sodium chloride (Vekton, Saint Petersburg, Russia) were used.

Preparation of Bacterial Cellulose Nanofibers

CNF were obtained according to a previously developed method.[48] Crushed BC (0.1 g) was dispersed in a mixture of ChCl (5.376 g) and urea (4.624 g). The ChCl-urea mixture was preliminarily heated at 90–95 °C in an oil bath until homogeneity was reached. Then BC was added and left for 90 min with permanent heating and stirring. After that, the dispersion of the CNF was washed with water by repeated centrifugations at a speed of 8000 r/min (Digisystem Laboratory Instruments Inc., New Taipei City, Taiwan) 15 min per cycle. The procedure of dispergation/centrifugation was repeated for at least 10 times to remove ChCl and urea residues.

Chemical Modification of Bacterial Cellulose Nanofibers

Dispersion of CNF was used as a raw material for modification. Grafting of poly(sodium acrylate-*co*-2-acrylamido-2-methylpropanesulfonic acid) (SA-AMPS) was performed on the surface of CNF using cerium (IV) ammonium nitrate ($(NH_4)_2Ce(NO_3)_6$) as initiator under optimal conditions found during preliminary studies (see Table S1 in the electronic supplementary information, ESI). In the case of optimal conditions AA (1.296 g) was mixed with equimolar amount of NaOH (0.72 g) and 2 mL of H_2O in a beaker at room temperature. Then AMPS was dissolved in 8 mL of H_2O and added to the solution of sodium acrylate in amount of 8.694 g. A solution of 0.2467 g of $(NH_4)_2Ce(NO_3)_6$ and 0.355 g of HNO_3 was prepared in 2 mL of H_2O and added to 7.5 g the CNF dispersion (2 wt%). Then the solution of monomers was added. The polymerization was carried out at 60 °C for 4 h. The resulting mixture was kept for 12 h at room temperature. The product was purified from not-grafted acrylic polymer by repeating of the dispersion-centrifugation procedures at least 10 times at a speed of 6000 r/min.

Preparation of Membranes from Modified Bacterial Cellulose

The obtained dispersions were diluted with water in order to attain a 0.3 wt% concentration of CNF(M). Sodium chloride (NaCl) as an agent for regulation of porosity[49,50] was added to the CNF(M) dispersion in an amount of 0%–20% respectively to the weight of CNF(M). The mixture was stirred for 1 day, casted on Petri dishes and dried at room temperature for 5–7 days. The obtained membranes were washed several times with water to remove salt and dried again until a constant mass was reached. In the text, they will be denoted as CNF(M)-0, CNF(M)-5, CNF(M)-10, CNF(M)-20 where the number denotes NaCl content in membrane. CNF(M)-0 and CNF(M)-20 samples were chosen as non-porous and the most porous membranes for major part of the studies. The membrane prepared from unmodified CNF was also prepared and studied for comparison.

The densities of prepared membranes were calculated from their mass measured gravimetrically using an AP225WD

(Shimadzu, Kyoto, Japan) microbalance using pieces 20 nm × 20 mm and measured thickness that was 16–24 μm. The porosity (P) of membranes was estimated from density measurements as $P = 100 \times (\rho_{non\text{-}p} - \rho_p)/\rho_{non\text{-}p}$, where $\rho_{non\text{-}p}$ is the density of non-porous film (CNF(M)-0 in our case) and ρ_p is the density of porous one.

Spectroscopy Study

Chemical structures of CNF and CNF(M) were characterized using IRAffinity-1S spectrometer (Shimadzu, Kyoto, Japan), in attenuated total reflectance (ATR) mode, with a scan range from 4000 cm^{-1} to 600 cm^{-1}. A total of 100 scans were made with a resolution of 2 cm^{-1}. Additional information was obtained using ^{13}C-NMR study using AVANCE II-500 WB NMR Fourier Spectrometer (Bruker, Germany).

Microscopic Investigation

Atomic force microscopy (AFM) studies were performed using SPM-9700HT scanning probe microscope (Shimadzu, Kyoto, Japan) in the tapping mode. NSG30-SS silicon cantilevers with a probe radius of 2 nm were used. Scanning electron microscopy (SEM) images of the membranes' surfaces were obtained with SUPRA 55 VP microscope (Carl Zeiss, Oberkochen, Germany) at voltage of 5 kV. Content of $-SO_3H$ groups in the CNF(M) was determined with energy dispersive X-ray (EDX) spectroscopy using Aztec Energy X-act microanalysis system (Oxford Instruments, UK) of Tescan Vega III SEM microscope (Tescan, Brno-Kohoutovice, Czech Republic). Transmission electron microscopy (TEM) studies were performed using JEM-2200 FS (JEOL, Japan).

Wide-angle X-ray Diffraction Study

The crystalline structure of the CNF and CNF(M) was studied *via* wide-angle X-ray diffraction (WAXD) with Rigaku SmartLab 3 diffractometer (Rigaku Corporation, Tokyo, Japan) equipped with CuK_α radiation source (λ=1.54 Å) within the 2θ range of 5°–40° with the scan step of 0.05°.

Measurement of Water Sorption Isotherms of Membranes

Sorption isotherms of the membranes were determined gravimetrically at room temperature. Six saturated salt solutions were selected, $CaCl_2$, $NaNO_3$, $MnCl_2$, NaCl, KCl and K_2SO_4 (RH=38%, 56.3%, 62.6%, 84.9%, 88.3% and 96.2%, respectively). RH value was controlled with an IVTM-7 K thermohygrometer (Moscow, Russia). The membranes were dried under vacuum at 60 °C for 7 days before experiments to remove residual moisture. Samples were placed in preliminarily weighed plastic sorption jars, and then kept inside desiccators with fixed RH. Masses of membranes were measured every 24 h until the constant values were reached. The amount of absorbed water was calculated and sorption isotherms were plotted. The Laatikainen-Lindstrom model[51] was used for fitting the sorption data. For this, the following equation was used:

$$a = a_m \frac{ah}{(1-\beta h)[1+(\alpha-\beta)h]} \quad (1)$$

where a_m and h are the concentration of primary sorption centers and the ratio of the partial pressure to the saturated vapor pressure. Based on α and β parameters the sorption on primary sorption centers (polar groups of polymer) and on secondary sorption centers (on previously sorbed water molecules, so called sorption in clusters) was estimated.

Mechanical Measurements

The stress-strain curves for the membranes were measured using the AG-100kNX Plus (Shimadzu, Japan) machine for mechanical measurements operating in the uniaxial extension mode. The ambient conditions during the experiment were 25 °C and 75% of relative humidity. Strip-like samples (2 mm × 15 mm) were clamped in the analyzer, and the load (N) and elongation (mm) were recorded with an extension velocity of 0.5 mm per minute. The values of Young's modulus, elongation at break and ultimate strain were obtained.

Electrochemical Measurements

All electrochemical measurements were conducted under the constant RH 98% using a climate chamber ERSTEVAK KTXB-64-D (Moscow, Russia) coupled with a P-40X potentiostat/galvanostat equipped with FRA24 impedance module (Elins, Moscow, Russia). The ionic conductivity of the membranes was studied over a range of temperatures 20–60 °C. The impedance spectra were acquired from 10 Hz to 100 kHz at voltage amplitude of 10 mV. Before measurement the membrane was soaked in distilled water or H_2SO_4 solution with concentration 1 $mol{\cdot}L^{-1}$. The membrane resistance (R) was determined from the high frequency intercept of the Nyquist plot with the axis of the real part of complex impedance. The through-plane conductivity σ ($mS{\cdot}cm^{-1}$) was calculated using the following equation:

$$\sigma = \frac{L}{RS} \quad (2)$$

where R is the electrical resistance, L is the membrane thickness and S is the electrode area.

In order to demonstrate practical applicability of prepared membranes, the model symmetric supercapacitor (SC) cell was built. For this purpose, the polyacrylamide-polyaniline (PAAm-PANI) based electrodes were prepared according to the method described earlier.[52] The SC was assembled by sandwiching of ICM between two electroactive polymer films that contain 0.89 mg of PANI each, and two pieces of organic glass covered with graphite foil as a current elector.

The electrochemical characteristics of prepared SC were investigated with cyclic voltammetry (CVA), galvanostatic charge-discharge (GCD), electrochemical impedance spectroscopy (EIS) and cycle stability measurements. The specific capacitance of SC was calculated from the discharge branch of GCD curves as $C_S = 2 \times It/(dU{\cdot}m)$, where I and t are the discharge current and duration, respectively; dU is the voltage range and m is the mass of active material on one electrode.

RESULTS AND DISCUSSION

Modification of CNF and Their Spectroscopic Characterization

It is known that $(NH_4)_2Ce(NO_3)_6$ is able to interact with organic compounds containing $-OH$ groups with formation of radicals on organic molecule that are able to initiate polymerization of acrylate monomers. The possible mechanisms of formation of such radical in the case of reaction with cellulose can be found elsewhere.[53,54] Thus, the successful grafting of polyacrylate onto cellulose surface using this initiator can be expected. During the preliminary study, the attempt of modification of CNF was

conducted with using of AMPS as a monomer and cerium(IV) ammonium nitrate initiator.

However, it is seen from ^{13}C-NMR results that the modification of cellulose did not happen: peaks corresponding to acrylic monomer cannot be found in NMR spectrum (see Fig. S1 in ESI). Only the peaks corresponding to cellulose at 102–108 (C_1), 80–92 (C_4), 70–80 (C_2, C_3 and C_5), 57–67 ppm (C_6) are visible (see Fig. S1 in ESI, CNF(M1) sample). Carbon atoms in brackets denotes numbers of atoms in glycoside ring that correspond to the mentioned peaks according to literature.[55,56] It can be proposed that adsorption of AMPS monomer on cellulose surface in proper orientation does not take place and thus grafting is hampered. At the same time, it was earlier demonstrated by computer simulation that acrylate anions can adsorb on cellulose surface *via* formation of hydrogen bonds.[57] Thus, it was proposed, that SA as a comonomer can induce grafting of polyacrylate onto the cellulose. This assumption was confirmed by experiment. As it is seen in Fig. S1 (in ESI) and Fig. 1(a) in spectra for samples prepared with addition of SA the additional peaks appear in the regions 170–175 ppm and 20–30 ppm. The first one can be attributed to the C=O groups of acrylate and amide groups,[58] while the second one to the aliphatic groups in AMPS[59] and polyacrylate main chain. The number of preliminary samples with variation of AMPS and SA content in the reaction mixture were prepared using parameters of synthesis given in Table S1 (in ESI). Based in ^{13}C-NMR spectra the sample with most intensive polyacrylate peaks (CNF(M3) in Fig. S1 in ESI) was chosen for further investigation and membrane preparation (this sample is denoted as CNF(M) in the main text). It was confirmed with EDX that this sample contains the maximal amount of —SO_3H groups grafted to the surface of CNF – 0.63 mmol·g^{-1} (see Table S2 in ESI).

Additional study of chemical structure of modified CNF was performed with FTIR (Fig. 1b) and obtained results are in agreement with ^{13}C-NMR data. Along with the presence of peaks corresponding to the vibrations of glycoside ring and —OH groups, the FTIR spectrum of CNF(M) shows the bands at 1713 and 1547 cm^{-1}. These peaks can be attributed to the vibrations of a carboxyl group (—COOH) in the protonated and deprotonated form, respectively. An increase in the absorption intensity in the region around 1646 cm^{-1} can be attributed to the introduction of the amide group from AMPS.[60] Such changes in the spectrum indicate that, under chosen conditions, the BC surface is modified with a copolymer consisting of acrylate and AMPS units. The retaining of bands of the initial cellulose in CNF(M) indicates the preservation of the chemical structure of the inner layers of BC nanofibers.

Investigation of Morphology of CNF(M) and ICM

The detailed images of the internal structures of CNF and CNF(M) were investigated by TEM (see Fig. 2a and Fig. 2b, respectively). It is seen that width of initial CNF was about 15 nm. The oriented dark lines inside fibril can be attributed to ordered macromolecules in cellulose crystallites that demonstrates the high crystallinity of CNF. It is seen from Fig. 2(b) that modification of nanofibers leads to increase in thickness up to 40–50 nm.

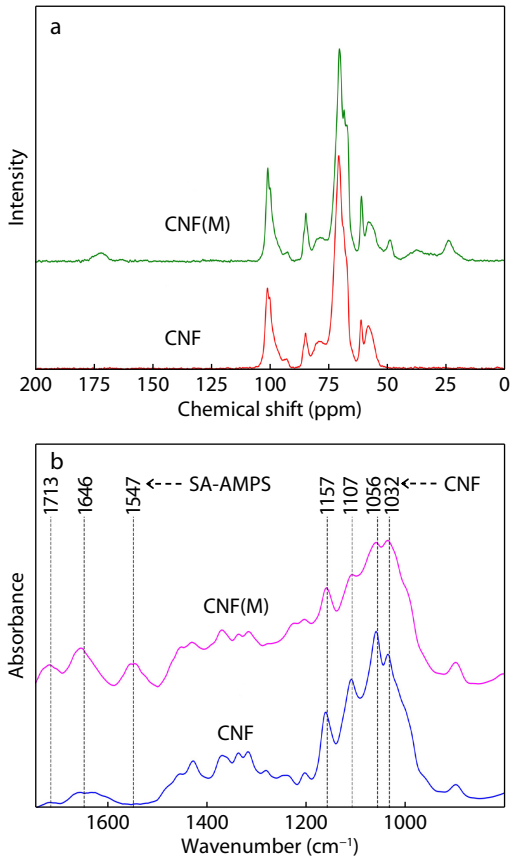

Fig. 1 (a) ^{13}C-NMR spectra and (b) FTIR spectra of initial CNF and CNF modified with a copolymer of SA and AMPS.

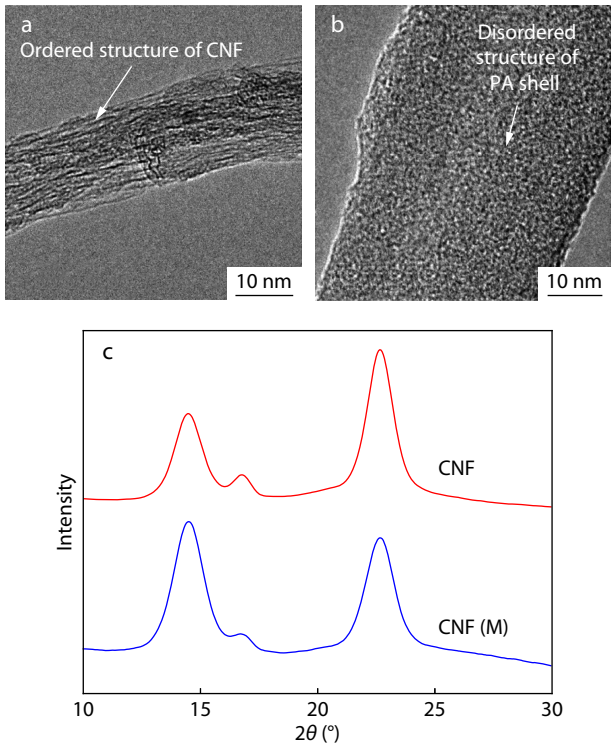

Fig. 2 TEM images for (a) initial and (b) modified CNF; (c) WAXD patterns for CNF and CNF(M).

https://doi.org/10.1007/s10118-023-3054-8

Additionally, the ordered structure of CNF(M) becomes completely masked by amorphous coating. This provides additional evidence for successful coating of CNF(M) with polyacrylate (PA) copolymer shell.

Fig. 2(c) shows the WAXD patterns of the initial CNF and CNF(M) that are typical for Cellulose I. Both patterns reveal three pronounced reflections that are attributed to the ordered structure of BC,[61] with intensity maxima at 2θ=14.5°, 16.7° and 22.7°. Thus the preservation of the crystalline structure of the cellulose after modification as it was proposed from NMR and FTIR study is confirmed.

The structure of ICM prepared by casting of CNF(M) dispersions was studied with SEM and AFM (Fig. 3). As can be seen in Figs. 3(a) and 3(c) the non-porous CNF(M)-0 membrane demonstrates dense homogeneous morphology and is characterized by the dense packing of the structural elements (nanofibers). The porous membrane prepared with addition of 20% NaCl in casting solution (CNF(M)-20) demonstrate a less dense packing of nanofibers and higher surface roughness (Figs. 3b and 3d) in comparison with CNF(M)-0. Space between fibers can be considered as pores. The porosity was calculated from membrane's density that was 1.34, 1.18 and 0.51 g·mL^{-1} for CNF(M)-0, membrane from unmodified CNF and CNF(M)-20, respectively. This allows to estimate porosity as 12% and 62% for membrane prepared from unmodified CNF and CNF(M)-20 that is in agreement with microscopy data. Slightly less dense structure for membranes prepared with pristine CNF in comparison with CNF(M)-0 is confirmed with SEM and AFM study (see Fig. S2 in ESI).

Measurement of Water Sorption Isotherms of ICM

Data on the water sorption activity of prepared ICM gives additional information about the physico-chemical properties of active sorption centers in polymer and behavior of materials under different humidity. The water sorption values of ICM at different RH were measured using the static gravimetric method (result is shown as points in Fig. 4). For a deeper discussion of the sorption experiment, the isotherms were fitted with a model developed for swellable polymers (especially cellulose) by Lindstrom and Laatikainen (LL isotherm).[51] Parameters of corresponding isotherm equation allow estimating the amount and activity of sorption sites and tendency of material to swell due to the formation of water clusters. The result of fitting of experimental data with the LL equation is shown in Fig. 4. Good correlation between experimental data and the model demonstrates its applicability to the process of water sorption in the membranes under study. The S-shaped curve of the isotherm can be attributed to the Langmuir type of sorption at low RH values with a continuous amount of active sorption centers—accessible polar groups of grafted polyacrylate. The progressive increase of sorption at high RH values demonstrates the appearance of the new sorption centers that can be secondary centers or primary sorption centers that become accessible due to swelling of grafted polyacrylate. In the case of membrane based on pristine CNF, sorption of water is the lowest at any RH. This demonstrates that polyacrylate shell significantly improves water sorption and retention of cellulose based ICM. These processes can be estimated qualitatively from refined parameters of LL isotherm that are given in Table 1.

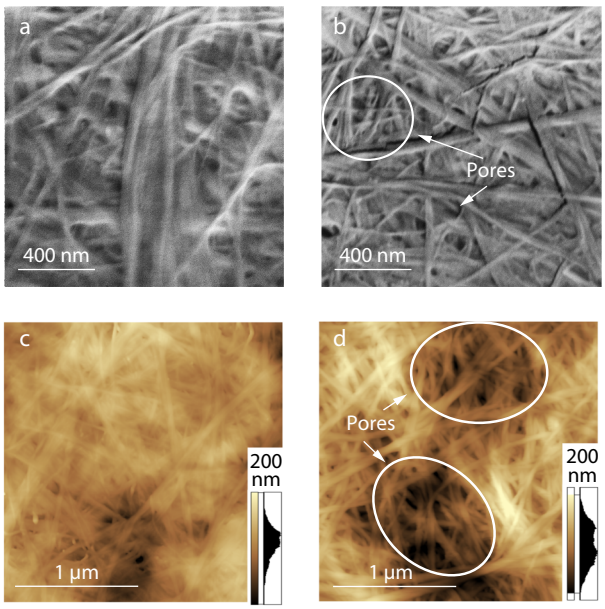

Fig. 3 SEM (a, b) and AFM images (c, d) for non-porous (a, c) and porous (b, d) ICM based on CNF(M).

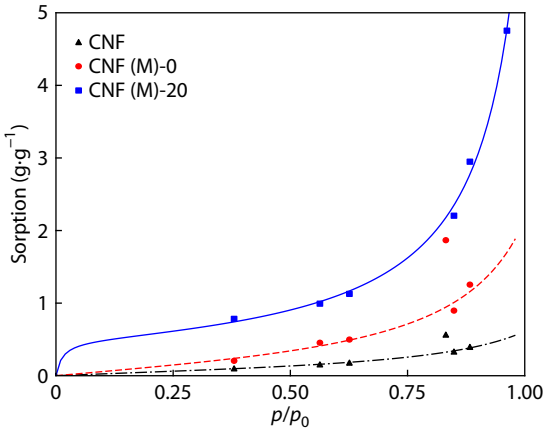

Fig. 4 Experimental values of water sorption for prepared ICM (points) and the result of their approximation by the LL isotherm (lines).

Table 1 Refined parameters of the Lindstrom-Laatikainen quasi-chemical model of water sorption in prepared ICM.

Sample	a_m	α	β
pristine CNF	0.1245	2.1125	0.8128
CNF(M)-0	0.3164	1.8167	0.8629
CNF(M)-20	0.4898	73.9812	0.9330

Higher values of parameter a_m for CNF(M)-20 membrane in comparison with CNF(M)-0 and membrane based on pristine CNF (Table 1) demonstrate an increase in number of accessible primary sorption centers that is connected with growth of pores sizes in ICM. Graphically this is depicted in Fig. 5(a) where sorption on active centers (ac) is given being calculated using refined parameters of LL model. Curve for CNF(M)-20 sample goes higher than for CNF(M)-0 and sorption on ac for

https://doi.org/10.1007/s10118-023-3054-8

porous sample reaches saturation at lower p/p_0 values. The value of the β describes the relative mobility of polymer chains, and it is the highest for CNF(M)-20 membrane. This means that more accessible free volume exists in CNF(M)-20 membrane due to pores and ability of grafted polyacrylate to swell. This free volume leads to the formation of clusters of water molecules and result in significant increasing of water sorption capacity of membrane especially at high values of p/p_0 as it can be seen in Fig. 5(b). This result allows to expect the highest ionic conductivity for CNF(M)-20 membranes and that will be demonstrated further.

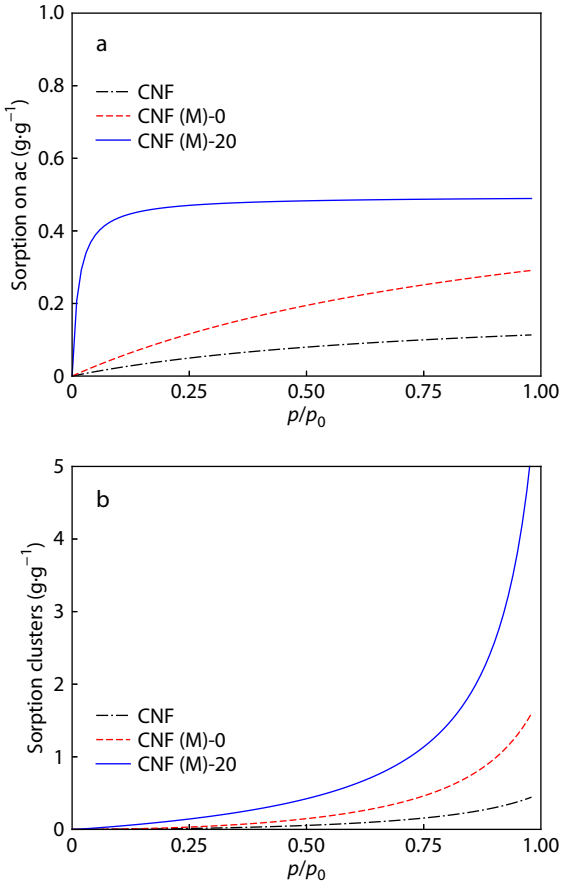

Fig. 5 Dependences of water sorption on the primary sorption centers of the polymer (a) and in clusters (b) on the activity of water vapor.

Mechanical Measurements

The stress-strain curves measured in uniaxial tension mode are shown in Fig. 6. It is seen that CNF(M)-0 and CNF(M)-20 membranes demonstrate 0.6% and 0.45% of elongation at break, respectively. Young's modulus decreases from 5.5 GPa for CNF(M)-0 to 1.1 GPa for CNF(M)-20 membrane. The strength decreases from 40 MPa for CNF(M) to 15 MPa for porous membrane. Decreasing of mechanical properties is connected with lowering of effective membrane cross-section due to formation of pores. Additionally, the density of contact between modified CNF decreases as it has been showing by AFM results discussed earlier. At the same time, the membrane prepared with nonmodified CNF demonstrated higher strength (76 MPa, see Fig. S3 in ESI) that can be attributed to higher strength of contacts between unmodified CNF due to cooperative hydrogen bonding of ordered cellulose surface. In spite of moderate mechanical characteristics of prepared ICM in comparison with reported in literature for other BC based membranes,[62–64] their strength was enough to manipulate with them easily during electrochemical studies and construction of model supercapacitor cell.

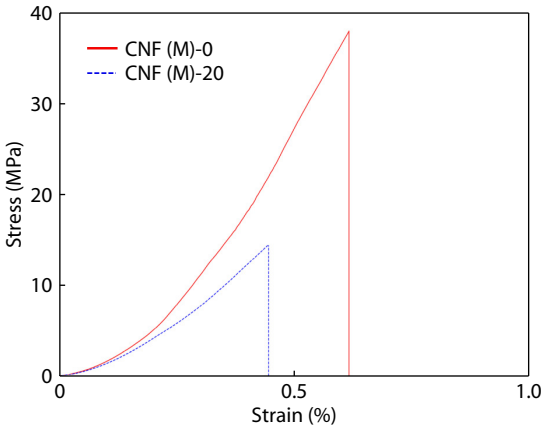

Fig. 6 Stress-strain curves for non-porous CNF(M)-0 and porous membrane CNF(M)-20.

Electrochemical Studies

Ionic conductivity

For measurement of electrochemical properties, prepared ICM were saturated with distilled water or with aqueous solution of H_2SO_4 (1 mol·L^{-1}). Throughout the following discussion, the corresponding membranes will be denoted as CNF(M)-*X*/H_2O and CNF(M)-*X*/H_2SO_4. The curves of the electrochemical impedance for obtained ICM are given in Fig. 7(a). It was found that ionic conductivity (σ) of non-porous CNF(M)-0/H_2O membrane is 0.17 mS·cm^{-1} at 25 °C. It is known from literature that neat BC is characterized by conductivity values ranging from 1.7×10^{-7} mS·cm^{-1} at 40 °C and 40% to 6.3×10^{-2} mS·cm^{-1} at 94 °C and 98%.[27,65] The membrane prepared from unmodified CNF in this work demonstrates ionic conductivity 0.09 mS·cm^{-1}. This demonstrates significant increasing of ionic conductivity of BC due to modification of CNF with selected acrylic copolymer. The formation of porous membranes leads to further increasing in ionic conductivity up to 0.83 mS·cm^{-1} for CNF(M)-20/H_2O at room temperature. This value is higher or comparable than for other membranes based on cellulose reported in literature, for example, 0.214 mS·cm^{-1} for microcrystalline cellulose modified with imidazole[66] and 1.2 mS·cm^{-1} for cellulose nanocrystals containing sulfosuccinic acid.[64]

Values of ionic conductivity of prepared ICM in a temperature range of 20–60 °C are given in Fig. S4 (in ESI). The maximal value obtained for CNF(M)-20/H_2O is 1.52 mS·cm^{-1} at 60 °C that is comparable to the values for ICM based on BC and fucoidan with conductivity 1.6 mS·cm^{-1}[67] and membrane based on carboxylated nanocellulose with 1.5 mS·cm^{-1}.[68] Obtained dependences of lg(σ) on 1/*T* are linear (Fig. 7b) that allows determination of activation energies of ionic conductivity (E_a). The result of the approximation is shown in Fig. 7(b) as lines and values of activation energies. It is found that E_a

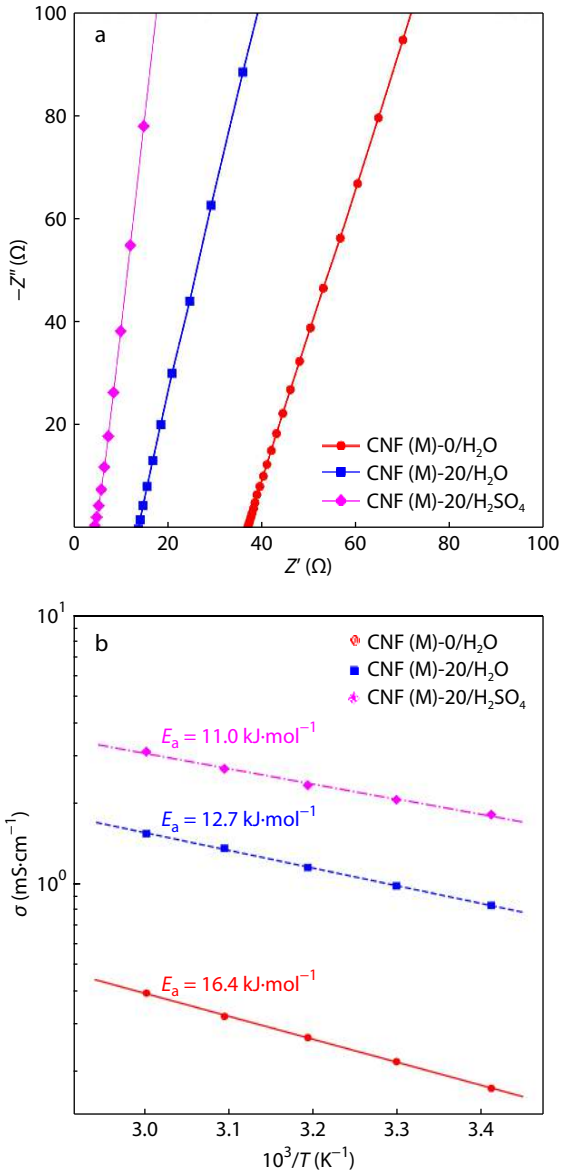

Fig. 7 Electrochemical impedance spectra for CNF(M)-0/H_2O, CNF(M)-20/H_2O and CNF(M)-20/H_2SO_4 (a) and dependencies of ionic conductivity of ICM on reciprocal temperature with determined activation energies of ionic conductivity (b).

decreases from 16.4 kJ·mol^{-1} for CNF(M)-0/H_2O to 12.7 kJ·mol^{-1} for CNF(M)-20/H_2O. Decreasing of E_a can be due to the increasing of polyacrylate chain mobility and water retention capacity as it was found from sorption experiments earlier. This can facilitate both vehicle and Grotthus mechanisms of proton transfer inside membrane. The obtained results are comparable to E_a reported in the literature for Nafion (10–20 kJ·mol^{-1})[69,70] and for membranes based on cellulose materials (10–30 kJ·mol^{-1}).[17]

In the case of CNF(M)-20/H_2SO_4 increase in ionic conductivity up to 1.79 mS·cm^{-1} at room temperature (about 2 times in comparison with water saturated ICM) and insignificant reduction of the activation energy down to 11.0 kJ·mol^{-1} were observed (Fig. 7b). This result allows us to propose that the charge transfer mechanism remains unchanged when water is replaced by acid and that the grafted ionogenic SA-AMPS copolymer dissociate inside the membrane, sufficiently to maintain the concentration of mobile ions in the membrane in the absence of external electrolyte.

Testing of model supercapacitor cell

For testing of model supercapacitor cell, the porous CNF(M)-20 membrane was soaked in the 1 mol·L^{-1} solution of H_2SO_4 or water and then sandwiched between two PAAm-PANI electrodes. The cell was initially tested by the CVA in the voltage range of 0–600 mV and at the scan rate from 10 mV·s^{-1} to 100 mV·s^{-1}. Measured currents were normalized by the mass of active material in the electrodes (PANI). It can be seen in Figs. 8(a) and 8(b) that compared with CNF(M)-20/H_2O, the CV curve of CNF(M)-20/H_2SO_4 covers a larger area, indicating that this cell has a higher specific capacitance. However, operation without external electrolyte, only with the internal dissociation of acrylic copolymer can be helpful in applications where the presence of hazardous acids is not allowed, for example in implantable electrochemical devices.[71] As the scanning rate increases, the oxidation peak gradually moves to the higher potential, while the reduction peak gradually shifts toward the lower potential because of the electrodes polarization. The CV curve maintains original shape even at a scan rate up to 1000 mV·s^{-1} (see Fig. S5 in ESI), indicating that the cell has good electrochemical reversibility. To evaluate the performance of prepared cells, the GCD analysis was performed. As it is seen in Figs. 8(c) and 8(d), GCD curves at the current density of 1 A·g^{-1} have a triangular shape showing an approximately linear dependence of potential on time that is characteristic of capacitance behavior. The results of impedance measurements are given in Fig. S6 (in ESI) and demonstrate that in both cases $-Z''$ (Z') plots show a nearly vertical line at low frequencies that also proves capacitance behavior of cells. The specific capacitance of SC with CNF(M)-20/H_2O and CNF(M)-20/H_2SO_4 reaches maximal values of 289 and 282 F·g^{-1}, respectively, at the current density of 1 A·g^{-1} (Fig. 8e). This is comparable to the reported values of 242 and 280 F·g^{-1} at a current density of 1 A·g^{-1} for the SC based on a carbon nanosheets framework with graphene hydrogel architecture derived from cellulose acetate[72] and based on three-dimensional carbonized polyimide/cellulose composite,[73] respectively. The increase of current density leads to decreasing of specific capacitance and maximal current at which GCD experiment could be performed was 20 A·g^{-1} for CNF(M)-20/H_2O-based cell. In these conditions, the cell demonstrates 239 F·g^{-1} of specific capacitance. At the same time, in the case of CNF(M)-20/H_2SO_4 the cell maintained operation at current densities up to 100 A·g^{-1}, the corresponding GCD curve is given in Fig. S7 (in ESI). This result is on the upper level between other ICM reported in literature. For example, in works,[74,75] maximal current densities were limited to 50 A·g^{-1}. The specific capacitance of model cell with CNF(M)-20/H_2SO_4 at current density 100 A·g^{-1} was 165 F·g^{-1} (Fig. 8e). Cyclic stability is an important electrochemical property for the practical application. Thus, cells with prepared ICM were subjected to the 10000 GCD cycles at a current density of 10 A·g^{-1}. Dependence of capacitance retention on the cycle number (see Fig. 8f) show that CNF(M)-20/H_2SO_4-based cell demonstrates some increase in capacitance retention from 500 cycles to 2500 cycles and a gradual decrease further. Capacitance retention remains 90% after 10000 cycles.

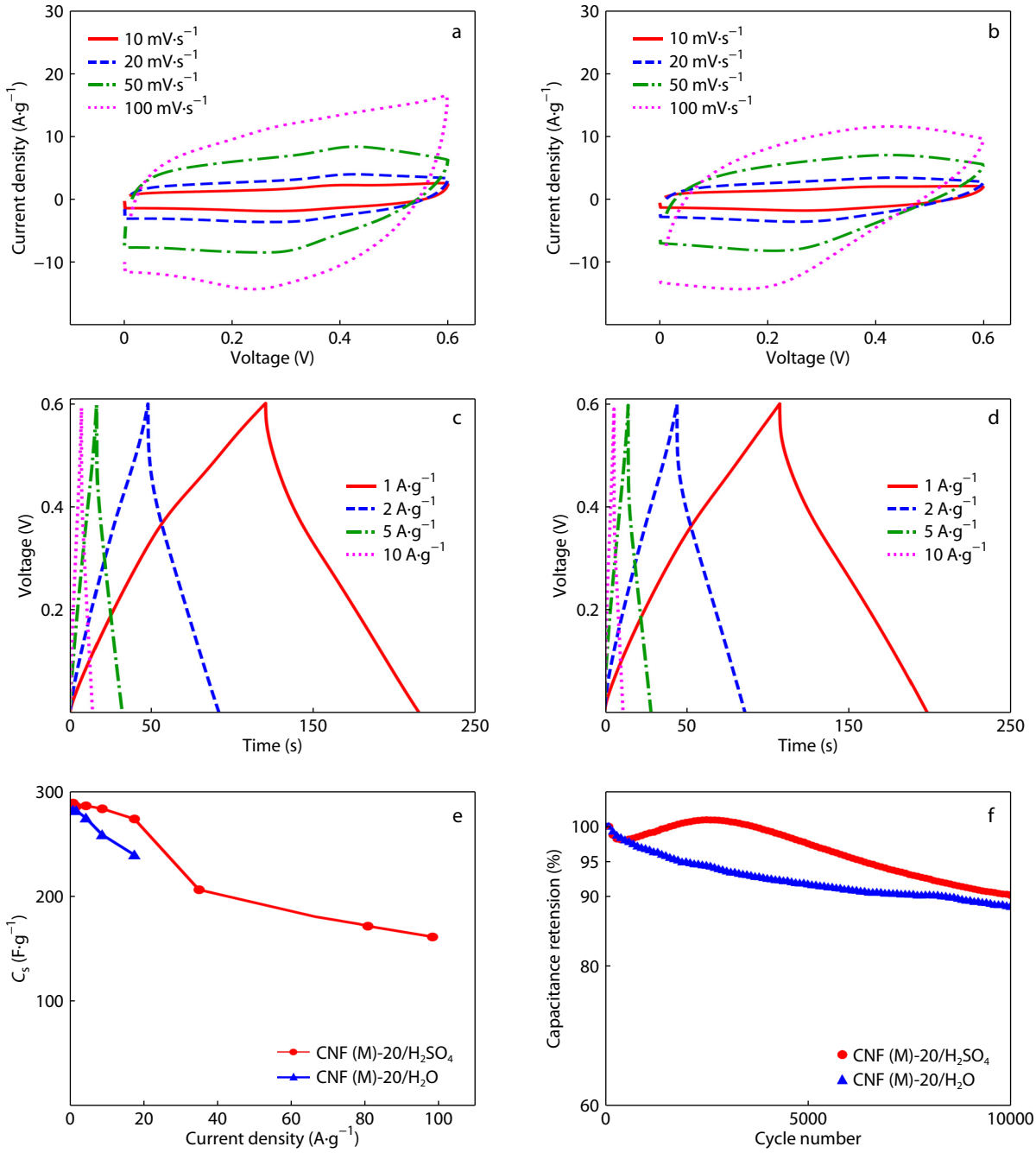

Fig. 8 CV curves of (a) CNF(M)-20/H_2SO_4-based and (b) CNF(M)-20/H_2O-based SC cells, GCD curves of (c) CNF(M)-20/H_2SO_4-based and (d) CNF(M)-20/H_2O-based SC cells, (e) dependences of specific capacitance on current density and (f) capacitance retention after GCD cycling at 10 A·g^{-1}.

It can be hypothesized that the increase in capacitance can be connected with hydrogel nature electroactive electrodes used for preparation of model cell in this study. In hydrogel state (being swollen with electrolyte) the electroconducting polymer chains are more mobile than in the case of solid porous electrode and thus conformational changes caused by chain movement during repetitive oxidation-reduction cycles can result in increasing availability of PANI chains for electrochemical reactions. The same effect was observed earlier for similar electrodes.[52,76] The further decreasing of capacitance is probably connected with overoxidation of PANI leading to the crosslinking of polymer and reduction of chain mobility, thus decreasing their electrochemical activity.[77] It can be noticed from Fig. 8(f), that for CNF(M)-20/H_2O -based cell, the gradual decrease starts from the beginning of the experiment. Thus, it can be proposed that neutral environment does not lead to the increasing of capacitance. It can be proposed that in acidic nature the PANI chains are more mobile because higher protonation leads to higher hydrophilicity (and thus swelling) of electroconducting hydrogel. At the

https://doi.org/10.1007/s10118-023-3054-8

same time, the residual capacitance after 10000 cycles is 88% that is only slightly lower than for CNF(M)-20/H_2SO_4. Obtained stability in both cases is higher than reported in literature (77.5%) after 3000 cycles,[78] 87% after 5000 cycles,[79] 86.8% after 10000 cycles[80] and 47% after 5000 cycles.[81]

CONCLUSIONS

The successful grafting of ionogenic acrylic copolymer on to the surface of CNF using cerium(IV) ammonium nitrate as initiator was demonstrated for the first time. The chemical structure of prepared nanomaterial was confirmed with NMR, FTIR and EDX studies. TEM results show the formation of an amorphous shell of polyacrylate onto a highly crystalline cellulose backbone. The possibility of preparation of self-standing porous ion-conducting membranes (ICM) *via* casting from dispersion of modified CNF was shown. Elaborated ICM had a high ionic conductivity up to 1.79 mS·cm^{-1} at room temperature and 3.1 mS·cm^{-1} at 60 °C due to porous structure and effective modification by grafting of ionogenic polyacrylate. In spite of moderate mechanical characteristics of prepared membranes, the self-standing properties were enough to use them as a separator in a symmetrical supercapacitor with polyacrylamide-polyaniline based electrodes. Due to high ion mobility and low activation energy of ionic conductivity, the supercapacitor cell based on prepared membranes demonstrated the possibility to operate at a high current density up to 100 A·g^{-1} maintaining 165 F·g^{-1} of specific capacitance. The maximal specific capacitance was achieved for CNF(M)-20/H_2SO_4-based cell: 289 F·g^{-1} at 1 A·g^{-1}. In addition, cells show very high electrochemical stability during 10000 of charge-discharge cycles with water or acidic electrolyte retaining 88% and 90% of initial capacitance, respectively.

Conflict of Interests

The authors declare no interest conflict.

Electronic Supplementary Information

Electronic supplementary information (ESI) is available free of charge in the online version of this article at http://doi.org/10.1007/s10118-023-3054-8.

ACKNOWLEDGMENTS

The work was carried out as part of a State Assignment 122012100170-1. Authors acknowledge shared facilities VTAN NSU for the usage of experimental equipment. The experimental work was also in part facilitated with equipment of the Engineering Center of St. Petersburg State Technological Institute (Technical University). Authors acknowledge Dr. N.N.Saprykina with the help in the scanning electron microscopy.

REFERENCES

1 de Oliveira, C. C. N.; Angelkorte, G.; Rochedo, P. R. R.; Szklo, A. The role of biomaterials for the energy transition from the lens of a national integrated assessment model. *Clim. Change* **2021**, *167*, 57.
2 Jian, M.; Zhang, Y.; Liu, Z. Natural biopolymers for flexible sensing and energy devices. *Chinese J. Polym. Sci.* **2020**, *38*, 459–490.
3 Wang, Y.; Ruiz Diaz, D. F.; Chen, K. S.; Wang, Z.; Adroher, X. C. Materials, technological status, and fundamentals of PEM fuel cells—a review. *Mater. Today* **2020**, *32*, 178–203.
4 Lizundia, E.; Kundu, D. Advances in natural biopolymer-based electrolytes and separators for battery applications. *Adv. Funct. Mater.* **2021**, *31*, 1–29.
5 Wang, S.; Zhang, L.; Zeng, Q.; Liu, X.; Lai, W. Y.; Zhang, L. Cellulose microcrystals with brush-like architectures as flexible all-solid-state polymer electrolyte for lithium-ion battery. *ACS Sustainable Chem. Eng.* **2020**, *8*, 3200–3207.
6 Wang, S.; He, J.; Li, Q.; Wang, Y.; Liu, C.; Cheng, T.; Lai, W. Y. Highly elastic energy storage device based on intrinsically super-stretchable polymer lithium-ion conductor with high conductivity. *Fundam. Res* **2022**, DOI: 10.1016/j.fmre.2022.06.003
7 Wang, S.; Bai, M.; Liu, C.; Li, G.; Lu, X.; Cai, H.; Liu, C.; Lai, W. Y. Highly stretchable multifunctional polymer ionic conductor with high conductivity based on organic-inorganic dual networks. *Chem. Eng. J.* **2022**, *440*, 135824.
8 Okonkwo, P. C.; Collins, E.; Okonkwo, E. Application of Biopolymer Composites in Super Capacitor, in *Biopolymer Composites in Electronics*, Elsevier, **2017**: bll 487–503.
9 Musa, M. T.; Shaari, N.; Kamarudin, S. K.; Wong, W. Y. Recent biopolymers used for membrane fuel cells: characterization analysis perspectives. *Int. J. Energy Res.* **2022**, *46*, 16178–16207.
10 Palanisamy, G.; Oh, T. H.; Thangarasu, S. Modified cellulose proton-exchange membranes for direct methanol fuel cells. *Polymers* **2023**, *15*, 639.
11 Winter, M.; Brodd, R. J. What are batteries, fuel cells, and supercapacitors. *Chem. Rev.* **2004**, *104*, 4245–4269.
12 Ng, W. W.; Thiam, H. S.; Pang, Y. L.; Chong, K. C.; Lai, S. O. A state-of-art on the development of nafion-based membrane for performance improvement in direct methanol fuel cells. *Membranes* **2022**, *12*, S06.
13 Xu, T. C.; Wang, C. S.; Hu, Z. Y.; Zheng, J. J.; Jiang, S. H.; He, S. J.; Hou, H. Q. High strength and stable proton exchange membrane based on perfluorosulfonic acid/polybenzimidazole. *Chinese J. Polym. Sci.* **2022**, *40*, 764–771.
14 Walkowiak-Kulikowska, J.; Wolska, J.; Koroniak, H. Biopolymer membranes in fuel cell applications, in *Biopolymer Membranes and Films*, Elsevier, **2020**: bll 423–476.
15 Bayer, T.; Cunning, B. V.; Šmíd, B.; Selyanchyn, R.; Fujikawa, S.; Sasaki, K.; Lyth, S. M. Spray deposition of sulfonated cellulose nanofibers as electrolyte membranes in fuel cells. *Cellulose* **2021**, *28*, 1355–1367.
16 Reddy, M. S. B.; Ponnamma, D.; Choudhary, R.; Sadasivuni, K. K. A comparative review of natural and synthetic biopolymer composite scaffolds. *Polymers* **2021**, *13*, 1105.
17 Selyanchyn, O.; Selyanchyn, R.; Lyth, S. M. A review of proton conductivity in cellulosic materials. *Front. Energy Res.* **2020**, *8*, 1–17.
18 Smirnov, M. A.; Sokolova, M. P.; Bobrova, N. V.; Toikka, A. M.; Morganti, P.; Lahderanta, E. Synergistic effect of chitin nanofibers and polyacrylamide on electrochemical performance of their ternary composite with polypyrrole. *J. Energy Chem.* **2018**, *27*, 843–853.
19 Vijayakumar, V.; Nam, S. Y. A review of recent chitosan anion exchange membranes for polymer electrolyte membrane fuel cells. *Membranes* **2022**, *12*, 1–12.
20 Vorobiov, V. K.; Smirnov, M. A.; Bobrova, N. V.; Sokolova, M. P. Chitosan-supported deep eutectic solvent as bio-based electrolyte for flexible supercapacitor. *Mater. Lett.* **2021**, *283*,

128889.
21 Wang, B.; Han, X.; Wang, Y.; Kang, L.; Yang, Y.; Cui, L.; Zhong, S.; Cui, X. Fabrication of alginate-based multi-crosslinked biomembranes for direct methanol fuel cell application. *Carbohydr. Polym.* **2023**, *300*, 120261.
22 Tiwari, T.; Srivastava, N. Exploring the possibility of starch-based electrolyte membrane in MFC application. *Macromol. Symp.* **2019**, *388*, 1–8.
23 Mohanapriya, S.; Rambabu, G.; Bhat, S. D.; Raj, V. Pectin based nanocomposite membranes as green electrolytes for direct methanol fuel cells. *Arab. J. Chem.* **2020**, *13*, 2024–2040.
24 Hernández-Flores, G.; Andrio, A.; Compañ, V.; Solorza-Feria, O.; Poggi-Varaldo, H. M. Synthesis and characterization of organic agar-based membranes for microbial fuel cells. *J. Power Sources* **2019**, *435*,
25 Kumar Gupta, P.; Sai Raghunath, S.; Venkatesh Prasanna, D.; Venkat, P.; Shree, V.; Chithananthan, C.; Choudhary, S.; Surender, K.; Geetha, K. An update on overview of cellulose, its structure and applications, in *Cellulose*, IntechOpen, **2019**: bll 1–21
26 Heinze, T.; El Seoud, O. A.; Koschella, A. Production and characteristics of cellulose from different sources, **2018**.
27 Gadim, T. D. O.; Loureiro, F. J. A.; Vilela, C.; Rosero-Navarro, N.; Silvestre, A. J. D.; Freire, C. S. R.; Figueiredo, F. M. L. Protonic conductivity and fuel cell tests of nanocomposite membranes based on bacterial cellulose. *Electrochim. Acta* **2017**, *233*, 52–61.
28 Batishcheva, E. V.; Sokolova, D. N.; Fedotova, V. S.; Sokolova, M. P.; Nikolaeva, A. L.; Vakulyuk, A. Y.; Shakhbazova, C. Y.; Ribeiro, M. C. C.; Karttunen, M.; Smirnov, M. A. Strengthening cellulose nanopaper *via* deep eutectic solvent and ultrasound-induced surface disordering of nanofibers. *Polymers* **2022**, *14*, 78.
29 Wang, Y.R.; Yin, C.C.; Zhang, J.M.; Wu, J.; Yu, J.; Zhang, J. Functional cellulose materials fabricated by using ionic liquids as the solvent. *Chinese J. Polym. Sci.* **2023**, *41*, 483–499.
30 Lin, D.; Liu, Z.; Shen, R.; Chen, S.; Yang, X. Bacterial cellulose in food industry: current research and future prospects. *Int. J. Biol. Macromol.* **2020**, *158*, 1007–1019.
31 Smirnov, M. A.; Fedotova, V. S.; Sokolova, M. P.; Nikolaeva, A. L.; Elokhovsky, V. Y.; Karttunen, M. Polymerizable choline-and imidazolium-based ionic liquids reinforced with bacterial cellulose for 3D-printing. *Polymers* **2021**, *13*, 3044.
32 Sathish, S.K.; Vitta, S. *Bacterial Cellulose Based Nanocomposites for Electronic and Energy Applications*. Elsevier. **2020**.
33 Ramírez-Carmona, M.; Gálvez-Gómez, M.P.; González-Perez, L.; Pinedo-Rangel, V.; Pineda-Vasquez, T.; Hotza, D. Production of bacterial cellulose hydrogel and its evaluation as a proton exchange membrane. *J. Polym. Environ*. **2023**, *31*, 2462–2472.
34 Smirnov, M. A.; Vorobiov, V. K.; Sokolova, M. P.; Bobrova, N. V.; Lahderanta, E.; Hiltunen, S.; Yakimansky, A. V. Electrochemical properties of supercapacitor electrodes based on polypyrrole and enzymatically prepared cellulose nanofibers. *Polym. Sci. - Ser. C.* **2018**, *60*, 228–239.
35 Shu, Y.; Bai, Q.; Fu, G.; Xiong, Q.; Li, C.; Ding, H.; Shen, Y.; Uyama, H. Hierarchical porous carbons from polysaccharides carboxymethyl cellulose, bacterial cellulose, and citric acid for supercapacitor. *Carbohydr. Polym.* **2020**, *227*, 115346.
36 Lahiri, D.; Nag, M.; Dutta, B.; Dey, A.; Sarkar, T.; Pati, S.; Edinur, H. A.; Kari, Z. A.; Noor, N. H. M.; Ray, R. R. Bacterial cellulose: production, characterization and application as antimicrobial agent. *Int. J. Mol. Sci.* **2021**, *22*, 1–18.
37 Mishra, S.; Singh, P. K.; Pattnaik, R.; Kumar, S.; Ojha, S. K.; Srichandan, H.; Parhi, P. K.; Jyothi, R. K.; Sarangi, P. K. Biochemistry, synthesis, and applications of bacterial cellulose: a review. *Front. Bioeng. Biotechnol.* **2022**, *10*, 1–12.
38 Jiang, G.; Zhang, J.; Qiao, J.; Jiang, Y.; Zarrin, H.; Chen, Z.; Hong, F. Bacterial nanocellulose/Nafion composite membranes for low temperature polymer electrolyte fuel cells. *J. Power Sources* **2015**, *273*, 697–706.
39 Gadim, T. D. O.; Vilela, C.; Loureiro, F. J. A.; Silvestre, A. J. D.; Freire, C. S. R.; Figueiredo, F. M. L. Nafion ® and nanocellulose: a partnership for greener polymer electrolyte membranes. *Ind. Crops Prod.* **2016**, *93*, 212–218.
40 Samaniego, A. J.; Espiritu, R. Prospects on utilization of biopolymer materials for ion exchange membranes in fuel cells. *Green Chem. Lett. Rev.* **2022**, *15*, 253–275.
41 Dahlström, C.; López Durán, V.; Keene, S. T.; Salleo, A.; Norgren, M.; Wågberg, L. Ion conductivity through TEMPO-mediated oxidated and periodate oxidated cellulose membranes. *Carbohydr. Polym.* **2020**, *233*, 115829.
42 Rana, H. H.; Park, J. H.; Gund, G. S.; Park, H. S. Highly conducting, extremely durable, phosphorylated cellulose-based ionogels for renewable flexible supercapacitors. *Energy Storage Mater.* **2020**, *25*, 70–75.
43 Yue, L.; Zheng, Y.; Xie, Y.; Liu, S.; Guo, S.; Yang, B.; Tang, T. Preparation of a carboxymethylated bacterial cellulose/polyaniline composite gel membrane and its characterization. *RSC Adv.* **2016**, *6*, 68599–68605.
44 Yue, L.; Xie, Y.; Zheng, Y.; He, W.; Guo, S.; Sun, Y.; Zhang, T.; Liu, S. Sulfonated bacterial cellulose/polyaniline composite membrane for use as gel polymer electrolyte. *Compos. Sci. Technol.* **2017**, *145*, 122–131.
45 Sriruangrungkamol, A.; Chonkaew, W. Modification of nanocellulose membrane by impregnation method with sulfosuccinic acid for direct methanol fuel cell applications. *Polym. Bull.* **2021**, *78*, 3705–3728.
46 Hao, Y.; Qu, J.; Tan, L.; Liu, Z.; Wang, Y.; Lin, T.; Yang, H.; Peng, J.; Zhai, M. Synthesis and property of superabsorbent polymer based on cellulose grafted 2-acrylamido-2-methyl-1-propanesulfonic acid. *Int. J. Biol. Macromol.* **2023**, *233*, 123643.
47 Anirudhan, T. S.; Rejeena, S. R. Poly(acrylic acid-*co*-acrylamide-*co*-2-acrylamido-2-methyl-1-propanesulfonic acid)-grafted nanocellulose/poly(vinyl alcohol) composite for the *in vitro* gastrointestinal release of amoxicillin. *J. Appl. Polym. Sci.* **2014**, *131*, 8657–8668.
48 Prosvirnina, A. P.; Bugrov, A. N.; Dobrodumov, A. V.; Vlasova, E. N.; Fedotova, V. S.; Nikolaeva, A. L.; Vorobiov, V. K.; Sokolova, M. P.; Smirnov, M. A. Bacterial cellulose nanofibers modification with 3-(trimethoxysilyl)propyl methacrylate as a crosslinking and reinforcing agent for 3D printable UV-curable inks. *J. Mater. Sci.* **2022**, *57*, 20543–20557.
49 Fager, C.; Gebäck, T.; Hjärtstam, J.; Röding, M.; Olsson, A.; Lorén, N.; von Corswant, C.; Särkkä, A.; Olsson, E. Correlating 3D porous structure in polymer films with mass transport properties using FIB-SEM tomography. *Chem. Eng. Sci. X.* **2021**, *12*, 100109.
50 Tessmar, J.; Holland, T.; Mikos, A. Salt Leaching for Polymer Scaffolds, in *Scaffolding In Tissue Engineering*, CRC Press, **2005**, bll 111–124
51 Laatikainen, M.; Lindstrom, M. General sorption isotherm for swelling materials. *Acta Polytech. Scand. Technol. Ser.* **1987**, *178*, 105–116.
52 Smirnov, M.A.; Sokolova, M.P.; Bobrova, N. V.; Kasatkin, I.A.; Lahderanta, E.; Elyashevich, G.K. Capacitance properties and structure of electroconducting hydrogels based on copoly(aniline-P-phenylenediamine) and polyacrylamide. *J. Power Sources* **2016**, *304*, 102–110.
53 Gaylord, N. Proposed new mechanism for catalyzed and uncatalyzed graft polymerization onto cellulose. *J. Polym. Sci., Part C: Polym Symp.* **1972**, *172*, 153–172.
54 Kalia, S.; Sabaa, M. W. in *Polysaccharide based graft copolymers*, SpringerLink, **2013**.
55 Jacek, P.; Kubiak, K.; Ryngajłło, M.; Rytczak, P.; Paluch, P.; Bielecki,

S. Modification of bacterial nanocellulose properties through mutation of motility related genes in Komagataeibacter hansenii ATCC 53582. *N. Biotechnol.* **2019**, *52*, 60–68.
56 Gelenter, M.D.; Wang, T.; Liao, S.Y.; O'Neill, H.; Hong, M. ^{2}H-^{13}C correlation solid-state NMR for investigating dynamics and water accessibilities of proteins and carbohydrates. *J. Biomol. NMR.* **2017**, *68*, 257–270.
57 Fedotova, V. S.; Sokolova, M. P.; Vorobiov, V. K.; Sivtsov, E. V.; Lukasheva, N. V.; Smirnov, M. A. Water influence on the physico-chemical properties and 3D printability of choline acrylate—bacterial cellulose inks. *Polymers* **2023**, *15*, 2156.
58 Porwal, S.; Diwedi, A.; Kamal, M.^{13}C NMR and Raman studies of fullerene-based poly(acrylamides). *Int. J. Org. Chem.* **2012**, *02*, 377–386.
59 Devrim, Y. G.; Rzaev, Z. M. O.; Pişkin, E. Synthesis and characterization of poly[((maleic anhydride)-*alt*-styrene)-*co*-(2-acrylamido-2-methyl-1-propanesulfonic acid)]. *Macromol. Chem. Phys.* **2006**, *207*, 111–121.
60 Qiao, J.; Hamaya, T.; Okada, T. New highly proton-conducting membrane poly(vinylpyrrolidone) (PVP) modified poly(vinyl alcohol)/2-acrylamido-2-methyl-1-propanesulfonic acid (PVA-PAMPS) for low temperature direct methanol fuel cells (DMFCs). *Polymer* **2005**, *46*, 10809–10816.
61 Mondal, M. I. H. Mechanism of structure formation of microbial cellulose during nascent stage. *Cellulose* **2013**, *20*, 1073–1088.
62 Jiang, G.; Qiao, J.; Hong, F. Application of phosphoric acid and phytic acid-doped bacterial cellulose as novel proton-conducting membranes to PEMFC. *Int. J. Hydrogen Energy.* **2012**, *37*, 9182–9192.
63 Ni, C.; Wang, H.; Zhao, Q.; Liu, B.; Sun, Z.; Zhang, M.; Hu, W.; Liang, L. Crosslinking effect in nanocrystalline cellulose reinforced sulfonated poly(aryl ether ketone) proton exchange membranes. *Solid State Ionics* **2018**, *323*, 5–15.
64 Selyanchyn, O.; Bayer, T.; Klotz, D.; Selyanchyn, R.; Sasaki, K.; Lyth, S. M. Cellulose nanocrystals crosslinked with sulfosuccinic acid as sustainable proton exchange membranes for electrochemical energy applications. *Membranes* **2022**, *12*, 658.
65 Gadim, T. D. O.; Figueiredo, A. G. P. R.; Rosero-Navarro, N. C.; Vilela, C.; Gamelas, J. A. F.; Barros-Timmons, A.; Neto, C. P.; Silvestre, A. J. D.; Freire, C. S. R.; Figueiredo, F. M. L. Nanostructured bacterial cellulose-poly(4-styrene sulfonic acid) composite membranes with high storage modulus and protonic conductivity. *ACS Appl. Mater. Interfaces.* **2014**, *6*, 7864–7875.
66 Bagus Pambudi, A.; Priyangga, A.; Hartanto, D.; Atmaja, L. Fabrication and characterization of modified microcrystalline cellulose membrane as proton exchange membrane for direct methanol fuel cell. *Mater. Today Proc.* **2020**, *46*, 1855–1859.
67 Vilela, C.; Silva, A. C. Q.; Domingues, E. M.; Gonçalves, G.; Martins, M. A.; Figueiredo, F.M.L.; Santos, S. A. O.; Freire, C. S. R. Conductive polysaccharides-based proton-exchange membranes for fuel cell applications: the case of bacterial cellulose and fucoidan. *Carbohydr. Polym.* **2020**, *230*, 115604.
68 Guccini, V.; Carlson, A.; Yu, S.; Lindbergh, G.; Lindström, R. W.; Salazar-Alvarez, G. Highly proton conductive membranes based on carboxylated cellulose nanofibres and their performance in proton exchange membrane fuel cells. *J. Mater. Chem. A* **2019**, *7*, 25032–25039.
69 Eikerling, M.; Kornyshev, A. A. Proton transfer in a single pore of a polymer electrolyte membrane. *J. Electroanal. Chem.* **2001**, *502*, 1–14.
70 Vayenas, C. G.; Tsampas, M. N.; Katsaounis, A. First principles analytical prediction of the conductivity of Nafion membranes. *Electrochim. Acta* **2007**, *52*, 2244–2256.
71 Zhou, J.; Zhang, R.; Xu, R.; Li, Y.; Tian, W.; Gao, M.; Wang, M.; Li, D.; Liang, X.; Xie, L.; Liang, K.; Chen, P.; Kong, B. Super-assembled hierarchical cellulose aerogel-gelatin solid electrolyte for implantable and biodegradable zinc ion battery. *Adv. Funct. Mater.* **2022**, *32*, 2111406.
72 An, Y.; Yang, Y.; Hu, Z.; Guo, B.; Wang, X.; Yang, X.; Zhang, Q.; Wu, H. High-performance symmetric supercapacitors based on carbon nanosheets framework with graphene hydrogel architecture derived from cellulose acetate. *J. Power Sources* **2017**, *337*, 45–53.
73 Li, H.; Cao, L.; Zhang, H.; Tian, Z.; Zhang, Q.; Yang, F.; Yang, H.; He, S.; Jiang, S. Intertwined carbon networks derived from polyimide/cellulose composite as porous electrode for symmetrical supercapacitor. *J. Colloid Interface Sci.* **2022**, *609*, 179–187.
74 Chen, L. F.; Huang, Z. H.; Liang, H. W.; Guan, Q. F.; Yu, S. H. Bacterial-cellulose-derived carbon nanofiber@MnO_2 and nitrogen-doped carbon nanofiber electrode materials: An asymmetric supercapacitor with high energy and power density. *Adv. Mater.* **2013**, *25*, 4746–4752.
75 Li, K.; Li, P.; Sun, Z.; Shi, J.; Huang, M.; Chen, J.; Liu, S.; Shi, Z.; Wang, H. All-cellulose-based quasi-solid-state supercapacitor with nitrogen and boron dual-doped carbon electrodes exhibiting high energy density and excellent cyclic stability. *Green Energy Environ.* **2022**, *8*, 1091–1101.
76 Smirnov, M. A.; Tarasova, E. V.; Vorobiov, V. K.; Kasatkin, I. A.; Mikli, V.; Sokolova, M. P.; Bobrova, N. V.; Vassiljeva, V.; Krumme, A.; Yakimanskiy, A. V. Electroconductive fibrous mat prepared by electrospinning of polyacrylamide-*g*-polyaniline copolymers as electrode material for supercapacitors. *J. Mater. Sci.* **2019**, *54*, 4859–4873.
77 Smirnov, M. A.; Vorobiov, V. K.; Kasatkin, I. A.; Vlasova, E. N.; Sokolova, M. P.; Bobrova, N. V. Long-term electrochemical stability of polyaniline- and polypyrrole-based hydrogels. *Chem. Pap.* **2021**, *75*, 5103–5112.
78 Sun, Z.; Thielemans, W. Interconnected and high cycling stability polypyrrole supercapacitors using cellulose nanocrystals and commonly used inorganic salts as dopants. *J. Energy Chem.* **2023**, *76*, 165–174.
79 Tanguy, N. R.; Wu, H.; Nair, S. S.; Lian, K.; Yan, N. Lignin cellulose nanofibrils as an electrochemically functional component for high-performance and flexible supercapacitor electrodes. *ChemSusChem.* **2021**, *14*, 1057–1067.
80 Sun, Y.; Yang, Y.; Fan, L.; Zheng, W.; Ye, D.; Xu, J. Polypyrrole/$SnCl_2$ modified bacterial cellulose electrodes with high areal capacitance for flexible supercapacitors. *Carbohydr. Polym.* **2022**, *292*, 119679.
81 Smirnov, M. A.; Sokolova, M. P.; Geydt, P.; Smirnov, N. N.; Bobrova, N. V.; Toikka, A. M.; Lahderanta, E. Dual doped electroactive hydrogelic fibrous mat with high areal capacitance. *Mater. Lett.* **2017**, *199*, 192–195.

https://doi.org/10.1007/s10118-023-3054-8